COMMUNICATION

OBC
www.rsc.org/obc

Ring-strain effects on the oxidation potential of enediynes and enediyne complexes

Kim K. Baldridge,[*a,b] **Bernadette T. Donovan-Merkert,**[*c] **Joseph M. O'Connor,**[*a] **Linda I. Lee,**[a] **Adam Closson,**[a] **Daniel Fandrick,**[a] **Tuan Tran,**[a] **Kevin D. Bunker,**[a] **Mouffouk Fouzi**[c] **and Peter Gantzel**[a]

[a] *Department of Chemistry and Biochemistry, University of California at San Diego, La Jolla, California 92093-0358, USA. E-mail: jmoconno@ucsd.edu; Fax: 858 534 5383; Tel: 858 534 5836*

[b] *San Diego Supercomputer Center, La Jolla, California 92093-0505, USA*

[c] *Department of Chemistry, University of North Carolina, Charlotte, North Carolina USA*

Received 26th September 2002, Accepted 28th January 2003
First published as an Advance Article on the web 12th February 2003

The metal–enediyne complexes [(η^5-C_5H_5)Fe{η^5-1,2-$C_5H_3C{\equiv}C(CH_2)_nC{\equiv}C$}] (4, *n* = 4; 5, *n* = 5) and [(η^5-C_5H_5)Fe{η^5-1,2-$C_5H_3(C{\equiv}CMe)_2$}] (6) were prepared from 1,2-diethynylferrocene (3). Complexes 4 and 5 were characterized in the solid state by X-ray crystallographic analysis. The structures of 4 and 6 were determined by computation using *ab initio* methods. A correlation was observed between ring-strain and increased ease of electrochemical oxidation along the series 6 (+0.164 V) to 5 (+0.152 V) to 4 (+0.123 V). A similar trend in ionization potentials was identified in both the gas phase and in solution by computational methods.

The effect of cycloalkyl-annelation on the structure, properties, and reactivity of aromatic rings has attracted the attention of organic chemists for over 50 years.[1,2] A particularly fascinating aspect of strained-ring annelation is the observation that the oxidation potentials within a series of naphthalenes becomes more positive as ring-strain is increased. To illustrate, oxidation of 1,2-dihydrocyclobuta[*b*]naphthalene (**1**, $E_{½}$ = + 1.59 V *vs.* SCE) occurs at 50 mV more positive potential than for 2,3-dimethylnaphthalene (**2**, $E_{½}$ = +1.54 V; Fig. 1).[2a] This, and related phenomena, have been attributed to a strain-induced rehybridization of the ring-junction carbons (*).[1,2] Thus, ring-strain results in increased p-character in the atomic orbitals used in the strained-ring and, conversely, increased s-character in the atomic orbitals used to form the sigma bond to the sp²-carbon α to the strained-ring.

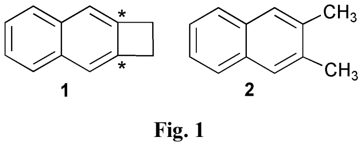

Fig. 1

Enediynes are of great interest due to the potent antitumor activity exhibited by naturally occurring strained-ring enediynes,[3] and the widespread use of enediynes as important units for the construction of carbon-rich systems.[4] Strained-ring alkynes have been widely studied from the perspective of reactions at the alkyne π-system;[5] however, the influence of cycloalkynyl-annelation on redox behaviour has not previously been reported. Here we report synthetic, electrochemical, and computational studies which establish a relationship between enediyne ring-strain and the electronic properties of enediynes and enediyne–metal complexes.

Sequential treatment of a THF solution (125 mL) of 1,2-diethynylferrocene[6] (**3**; 383 mg, 1.64 mmol) with *n*-BuLi (4.1 mmol) and 1,4-diiodobutane (0.54 g, 1.64 mmol) gave the enediyne complex [(η^5-C_5H_5)Fe{η^5-1,2-$C_5H_3C{\equiv}C(CH_2)_4C{\equiv}C$}] (**4**) as a yellow–orange air-stable solid in 26% yield (Scheme 1).[7–9] The 11-membered ring analogue **5** and the acyclic dipropynyl analogue **6** were prepared from **3** in a similar fashion. A DEPT NMR spectrum ($CDCl_3$) of **4** supports the assignment of carbon resonances at δ 80.0 and 96.2 to the alkyne sp-carbons. For comparison, the alkyne carbons in **5** are observed at δ 80.2 and 91.8; whereas, for **6** these resonances are located farther upfield at 76.0 and 84.3. The ^{13}C NMR spectroscopic data are consistent with an increase in p-character at the alkyne–cyclopentadienyl bonds proceeding across the series from **6** to **5** to **4**.

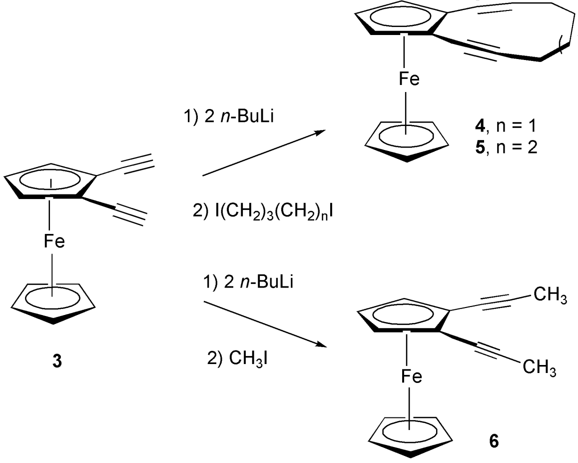

Scheme 1

The structural details for **3**–**6** were established by X-ray crystallography (**4**, **5**; Table 1; Fig. 2)[10] and by computation using *ab initio* methods (**4**, **6**; Table 1).[11] The validity of the computational results is supported by the remarkably close agreement between the crystallographic and computational data for **4** (Table 1). For the series of compounds **4**–**6**, the bond distances of the enediyne unit (*α*, *β*, *γ*) are similar within the experimental uncertainty; however, large geometric differences in the enediyne angles are observed along this series. Angular distortions at the proximal alkyne carbons in the 10-membered ring enediyne **4** are significantly greater (B = 163.5°) than at the distal alkyne carbons (C = 172.7°; 171.8° calc). In contrast, the B/C angles for the 11-membered ring compound **5** are 168.6° and 171.0°, respectively. Both **4** and **5** fit the structural criteria for angle-strained alkynes,[7] with the average angle about the sp-carbons bound to the Cp-ring in **4** and **5** determined to be 163° and 168°, respectively. The *cd*-distance in **4** (3.4 Å, 3.5 Å calc) and in **5** (3.8 Å) is significantly shorter than the corresponding distance calculated for **6** (4.6 Å).

DOI: 10.1039/b209285a

Table 1 Bond lengths (Å), angles (°) for **4**, **5** and **6**

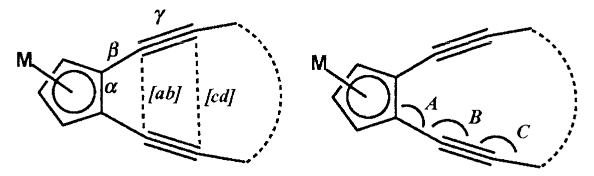

Compound	**6**(calc)	**5**	**4**	**4**(calc)
[ab]	3.15	2.94	2.86	2.90
[cd]	4.59	3.78	3.39	3.48
α	1.463	1.446(7)	1.451(8)	1.469
β	1.426	1.423(7) 1.414(7)	1.436(9) 1.427(9)	1.426
γ	1.224	1.184(8) 1.190(8)	1.171(8) 1.194(9)	1.226
A	126.3	122.3(5) 121.5(5)	119.7(6) 119.1(6)	120.1
B	178.5	169.6(6) 167.7(7)	162.6(7) 164.4(7)	163.5
C	179.6	170.5(7) 171.6(8)	172.9(7) 172.5(6)	171.8

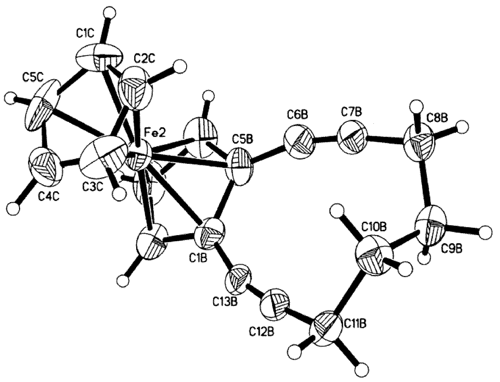

Fig. 2 ORTEP diagram for **4**-monoclinic. Selected bond lengths [Å] and angles [°]: C(1B)–C(13B) 1.435(9), C(1B)–C(5B) 1.436(9), C(2B)–C(3B) 1.412(9), C(3B)–C(4B) 1.418(10), C(4B)–C(5B) 1.415(9), C(5B)–C(6B) 1.434(10), C(6B)–C(7B) 1.206(9), C(7B)–C(8B) 1.465(9), C(11B)–C(12B) 1.473(9), C(12B)–C(13B) 1.188(9), C(1C)–C(2C) 1.362(10); C(13B)–C(1B)–C(5B) 120.0(6), C(7B)–C(6B)–C(5B) 162.6(7), C(6B)–C(5B)–C(1B) 120.2(6), C(6B)–C(7B)–C(8B) 172.4(7), C(13B)–C(12B)–C(11B) 172.9(7), C(12B)–C(13B)–C(1B) 163.1(7).

In order to establish the electronic effect of ring-strain on organometallic enediynes, cyclic voltammetry studies were performed on **3**–**6** in CH_3CN–0.1 M $TBAPF_6$.[12] For this series of complexes, a one-electron oxidation process is observed with $E_{1/2}$ values (*vs.* Fc/Fc$^+$) determined to be +0.294 V (**3**), +0.164 V (**6**), +0.152 V (**5**), and +0.123 V (**4**). The substantial electronic effect which occurs upon replacing a hydrogen by a methyl (in this case comparison of **3** and **6**) is well established. The observation that strained-ring enediyne **4** is 41 mV *easier* to oxidize than dipropynyl complex **6** runs counter to the previous observation that strained-ring compound **1** is 50 mV *more difficult* to oxidize than **2**. The 41 mV difference in oxidation potential between **4** and **6** is therefore a surprisingly large electronic effect.

The oxidation potential of numerous ferrocene derivatives has been shown to correlate with inductive substituent parameters.[13] In order to obtain a comparison of sp^3-, sp^2- and sp-hybridization on the oxidation potential of monosubstituted ferrocenes in CH_3CN–0.1 M $TBAPF_6$, we determined the oxidation potentials (*vs.* Fc/Fc$^+$) for ethylferrocene ($E_{1/2}$ = −0.056 V), ethenylferrocene ($E_{1/2}$ = +0.019 V) and ethynylferrocene ($E_{1/2}$ = +0.157 V). Thus, there is a 138 mV difference in oxidation potential between the ethenyl and ethynyl substituents.

Table 2 Ionization potential data (eV)

Gas phase, Koopmans'

Compound	B3LYP/SDD	Δ(IP)	B3LYP/DZ(2d,p)
1	−5.8450	0.0778	−5.7881
2	−5.7672		−5.7204
4	−5.4298	0.0071	
6	−5.4368		
7	1.9820	0.0067	
8	1.9888		

Gas phase, Δ(SCF)

Compound	B3LYP/SDD	Δ(IP)	B3LYP/DZ(2d,p)
1	−7.5427	0.0912	−7.5563
2	−7.6339		−7.4726
4	−6.0706	0.0015	
6	−6.0721		

Acetonitrile, Koopmans'

Compound	B3LYP/SDD	Δ(IP)	B3LYP/DZ(2d,p)
1	−5.9729	0.0718	−5.9049
2	−5.9011		−5.8406
4	−5.5813	0.0204	
6	−5.6017		

Acetonitrile, Δ(SCF)

Compound	B3LYP/SDD	Δ(IP)	B3LYP/DZ(2d,p)
1	−6.0829	0.0592	−5.9969
2	−6.0236		−5.9470

Computational methods were utilized to determine the ionization potentials for naphthalenes **1** and **2**; and cyclopentadienyl-iron complexes **4** and **6** (Table 2).[11] Results for **1** and **2** are shown for both B3LYP/DZ(2d,p) and B3LYP/SDD to help establish method reliability. Computational ionization energy values for all four structures result from Koopmans' theorem estimates as well as the more accurate Δ(SCF) method. The results are consistent with the experimental observations that dimethylnaphthalene **2** is easier to oxidize than ring-strained cycloalkyl **1**, whereas ring-strained **4** is easier to oxidize than **6**.

In addition to rehybridization effects, the change in oxidation potential along the series **6**–**4** could be influenced by an interaction of the alkyne π-system(s) directly with the iron center. Fig. 3 shows the molecular orbital contour plots for the HOMO of both **4** and **6**. In order to clarify the effect of the metal center on the ionization potential of **4** and **6**, we examined the metal-free cyclopentadienide-enediynes **7** and **8** (Fig. 4, Table 2). The remarkable similarity in Δ(IP) for **7** and **8** (0.0067 eV) compared to that for **4** and **6** (0.0071 eV) indicates that the differences in ionization potential across the series **4**–**6** are not due to the effects of metal–alkyne interactions.

Solvation calculations were also performed within the conductor-like screening model approximations[11j] at a relative permittivity of $\varepsilon = 36.64$, mimicking that of acetonitrile (used as the solvent in the electrochemical experiments) in order to observe the change in ionization potential with change in dielectric. Computational ionization energy values for all structures result from Koopmans' theorem estimates as well as the more accurate Δ(SCF) method.[11k] We note that similar trends are achieved for both methods, and therefore, for complexes **4** and **6** in solution, only the former was performed to conserve computational effort. The solution studies indicate a significant solvent effect on the difference in ionization potential for **4** and **6** (Δ(IP) = 0.020). The larger value of Δ(IP) in polar media relative to that in the gas phase may be attrib-

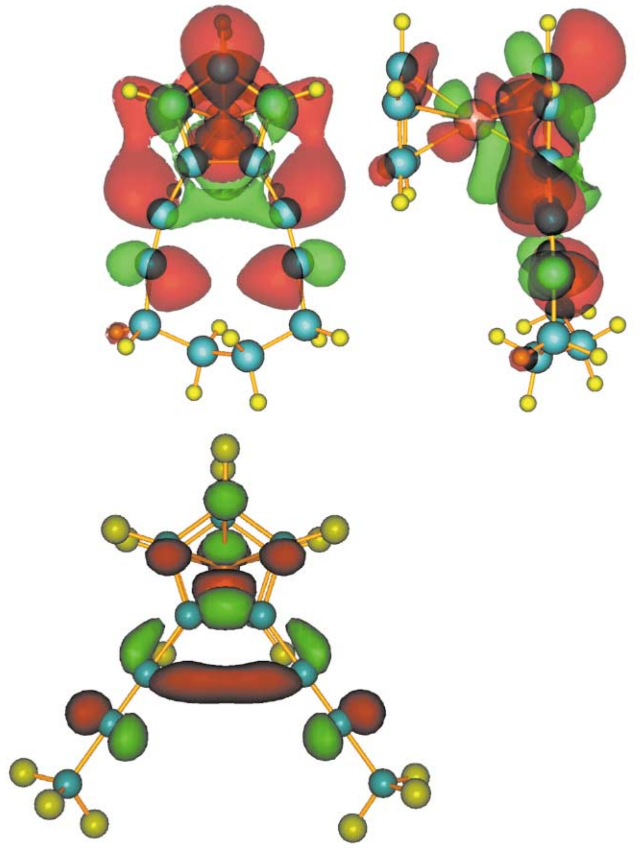

Fig. 3 Highest Occupied Molecular Orbital contour plots for **4** (top) and for **6** (bottom).[11h,i] Green and red colors indicate orbital lobes of opposite sign.

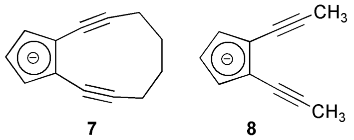

7 **8**

Fig. 4

uted to a larger dipole moment for ring-strained structure **4** (μ = 1.45 D) than for **6** (μ = 0.88 D).

The results reported herein establish a relationship between ring-strain and the electronic properties of conjugated enediynes and enediyne–metal complexes. The observed trend is in the opposite direction to that observed previously for oxidation of systems involving cycloalkyl ring-strain (*e.g.* **1**, **2**). A comparison of the trend observed for the naphthalenes to that observed for the iron complexes is complicated by the fact that the oxidation is metallocene-based in the latter and from the π-system in the former. However, the computational results in Table 2 indicate that ring-strain in the metal-free enediynes raises the energy of the HOMO (ring-strained **7** *vs.* **8**) by a similar magnitude to that observed in iron complexes (ring-strained **4** *vs.* **6**). Thus, the higher energy HOMO for the organic system (ligand) also increases the energy of the metallocene-based HOMO.

The correlation between ring-strain and the increased ease of oxidation along the series **6** < **5** < **4** is distinctly not due to differences in metal–enediyne interactions across the series. Furthermore, if rehybridization effects were the primary factor responsible for the observed trend, then one would have expected to see a similar effect in the organic systems. Thus, we suggest that the observed trends for **4**–**6** and **7**,**8** are primarily due to increased in-plane π–π repulsion as increased ring-strain brings the alkynes into closer proximity.[4c]

Acknowledgements

This work was supported by the National Science Foundation (JMO: CHE-9970480; BTD-M: CHE-9973668), the National Institutes of Health (KKB: NIH PA1 RR08615-06), the University of California Cancer Coordinating Committee (JMO), and the Henry Dreyfus Teacher-Scholar Awards Program (BTD-M). We are grateful for the allocation of supercomputer time from the NSF SDSC/NRAC program, and for helpful discussions with Professors Perrin and Siegel.

References

1 H.-D. Beckhaus, R. Faust, A. J. Matzger, D. L. Mohler, D. W. Rogers, C. Ruechardt, A. K. Sawhney, P. S. Verevkin, K. P. C. Vollhardt and S. Wolff, *J. Am. Chem. Soc.*, 2000, **122**, 7819; N. L. Frank and J. S. Siegel, *Adv. Theor. Interesting Mol.*, 1995, **3**, 209.

2 (*a*) R. D. Rieke, W. E. Rich and T. H. Ridgeway, *J. Am. Chem. Soc.*, 1971, **93**, 1962; (*b*) R. D. Rieke, S. E. Bales, C. F. Meares, L. I. Rieke and C. M. Milliren, *J. Org. Chem.*, 1974, **39**, 2276 and references therein; (*c*) A. Streitwieser, Jr. and D. M. E. Reuben, *J. Am. Chem. Soc.*, 1971, **93**, 1794 and references therein; (*d*) Z. Glasovac, M. Eckert-Maksic, K. M. Broadus, M. C. Hare and S. R. Kass, *J. Org. Chem.*, 2000, **65**, 1818 and references therein.

3 A. L. Smith and K. C. Nicolaou, *J. Med. Chem.*, 1996, **39**, 2103.

4 (*a*) M. B. Nielsen and F. Diederich, *The Chemical Record*, 2002, **2**, 189; (*b*) M. Laskoski, W. Steffen, J. G. M. Morton, M. D. Smith and U. H. F. Bunz, *Angew. Chem., Int. Ed.*, 2002, **41**, 2378; (*c*) R. Gleiter and W. Schäfer, *Acc. Chem. Res.*, 1990, **23**, 369.

5 (*a*) P. I. Dosa, C. Erben, V. S. Iyer, K. P. C. Vollhardt and I. M. Wasser, *J. Am. Chem. Soc.*, 1999, **121**, 10430; (*b*) H. N. C. Wong, *Adv. Theor. Interesting Mol.*, 1995, **3**, 209.

6 For non-strained ferrrocene-based enediynes, see: (*a*) U. H. F. Bunz, *J. Organomet. Chem.*, 1995, **494**, C8; (*b*) U. H. F. Bunz, G. Roidl, M. Altmann, V. Enkelmann and K. D. Shimizu, *J. Am. Chem. Soc.*, 1999, **121**, 10719.

7 To our knowledge, complex **4** is the first *strained*-ring enediyne in which the ene-function is incorporated into a five-membered ring. Ring-strained alkynes are defined as those with an average C–C≡C angle of *ca.* 10° or larger: A. Krebs and J. Wilke, *Top. Curr. Chem.*, 1983, **109**, 189.

8 For representative ene-coordinated enediynes: (*a*) J. M. O'Connor, L. I. Lee, P. Gantzel, A. L. Rheingold and K. C. Lam, *J. Am. Chem. Soc.*, 2000, **122**, 12057; (*b*) T. Haseqaga and L. Pu, *J. Organomet. Chem.*, 1997, **527**, 287; (*c*) U. H. F. Bunz, *Carbon Rich Compd. II*, 1999, **201**, 131; (*d*) J. R. Fritch and K. P. C. Vollhardt, *J. Am. Chem. Soc.*, 1978, **100**, 3643.

9 For **4**: mp 94–95 °C; ^1H NMR ($CDCl_3$, 500 MHz, δ): 1.94 (m, 4H), 2.30 (m, 4H), 4.06 (t, J = 2.5 Hz, 1H), 4.06 (s, 5H), 4.28 (d, J = 2.5 Hz, 2H); $^{13}C\{^1H\}$ NMR ($CDCl_3$, 125.7 MHz, δ): 21.6, 28.8, 66.9, 67.0, 71.5, 74.0, 80.0, 96.2; IR (NaCl, film, cm^{-1}): 3105, 2933, 2861, 2230; HRMS-EI (*m*/*z*): $[M]^+$ calcd for $FeC_{18}H_{16}$, 288.0601; found 288.0589.

10 Crystallographic data (excluding structure factors) have been deposited with the Cambridge Crystallographic Data Centre as supplementary publication nos. CCDC 170841 (**4**-monoclinic), CCDC 170842 (**4**-triclinic), and CCDC 170843 (**5**). See http://www.rsc.org/suppdata/ob/b2/b209285a/ for crystallographic files in .cif or other electronic format. Copies of the data can be obtained free of charge on application to CCDC, 12 Union Road, Cambridge, UK CB2 1EZ (Fax (+44)1223-336-033; E-mail: deposit@ccdc.cam.ac.uk).

11 (*a*) All calculations have been carried out using the Gaussian98[11b] and GAMESS[11c] software packages, running on the hardware facilities at the San Diego Supercomputer Center. The molecular structures were determined using a variety of levels of theory to establish self-consistency in terms of basis sets as well as effects of dynamic correlation. Hybrid density functional theory (HDFT) methods were primarily employed, using the Becke's 3 parameter hybrid exchange functional[11d] in combination with the nonlocal correlation functional provided by the Lee–Yang–Parr expression,[11e] B3LYP. Relativistic effective core potentials (SDD)[11f] were used for the transition metal, while all other atoms were treated with the Dunning–Huzinaga DZV(2d,p) basis set.[11g] The specific effective core potential–basis set combination used was the Stuttgart–Dresden-double-ζ basis set (6d, 10f). We show results for both B3LYP/DZ(2d,p) and B3LYP/SDD for the model system to help establish method reliability. Full geometry optimizations and

subsequent second derivatives analyses to confirm stationary point characters were performed. Molecular orbital contour plots, used as an aid in the discussion of the results, were generated using the program 3D-PLTORB,[11h] and depicted using QMView[11i]; (*b*) M. J. Frisch, G. W. Trucks, H. B. Schlegel, P. M. W. Gill, B. G. Johnson, M. A. Robb, J. R. Cheeseman, T. A. Keith, G. A. Petersson, J. A. Montgomery, K. Raghavachari, M. A. Al-Laham, V. G. Zakrzewski, J. V. Ortiz, J. B. Foresman, J. Cioslowski, B. B. Stefanov, A. Nanayakkara, M. Challacombe, C. Y. Peng, P. Y. Ayala, W. Chen, M. W. Wong, J. L. Andres, E. S. Replogle, R. Gomperts, R. L. Martin, D. J. Fox, J. S. Binkley, D. J. DeFrees, J. Baker, J. P. Stewart, M. Head-Gordon, C. Gonzalez, J. A. Pople, GAUSSIAN98-DFT; Revision D.3 ed.; Gaussian, Inc.: Pittsburgh, PA, 1998; (*c*) M. W. Schmidt, K. K. Baldridge, J. A. Boatz, S. T. Elbert, M. S. Gordon, J. H. Jensen, S. Koseki, N. Matsunaga, K. A. Nguyen, S. Su, T. L. Windus and S. T. Elbert, *J. Comput. Chem.*, 1993, **14**, 1347; (*d*) A. D. Becke, *J. Chem. Phys.*, 1993, **98**, 5648; (*e*) C. Lee, W. Yang and R. G. Parr, *Phys. Rev. B*, 1988, **37**, 785; (*f*) P. Fuentealba, H. Preuss, H. Stoll and L. V. Szentpaly, *Chem. Phys. Lett.*, 1989, **89**, 418; (*g*) T. H. Dunning, Jr., P. J. Hay, in *Modern Theoretical Chemistry*, Ed. H. F. Schaefer, III, Plenum, New York, 1976, vol. 3, p. 1; (*h*) *3D-PLTORB*: San Diego, 3D version: 1997; (*i*) K. K. Baldridge and J. P. Greenberg, *J. Mol. Graphics*, 1995, **13**, 63; (*j*) A. Klamt and G. Schüürmann, *J. Chem. Soc., Perkin Trans. 2*, 1993, 799; K. K. Baldridge and A. Klamt, *J. Chem. Phys.*, 1997, **106**, 6622; (*k*) For a discussion of Koopmans' theorem and Δ(SCF), see: T. Koopmans, *Physica*, 1934, **1**, 104; J. Almlof, B. Roos, U. Wahlgreen and H. Johansen, *J. Electron Spectrosc. Relat. Phenom.*, 1973, **2**, 51; K. D. Jordan and M. N. Paddon-Row, *J. Phys. Chem.*, 1992, **96**, 1188.

12 Cyclic voltammetry experiments were performed using an EG&G Princeton Applied Research model 273A potentiostat/galvanostat driven using the EG&G model 270/250 research electrochemistry software package. Cyclic voltammetry experiments employed a conventional three-electrode configuration using a glassy carbon disk working electrode, a platinum wire counter electrode, and a non-aqueous reference electrode consisting of a silver wire immersed in an acetonitrile solution of 0.1 M tetrabutylammonium hexafluorophosphate–0.01 M $AgNO_3$ separated from the rest of the cell by a Vycor frit. The scan rate employed for the reported potentials was 200 mV s^{-1}. The waves were determined to be chemically reversible ($i_c/i_a = 1$) and diffusion-controlled over a scan rate range of 50–500 mV s^{-1}.

13 (*a*) W. E. Geiger, *J. Organomet. Chem. Libr.*, 1990, **22**, 142; (*b*) S. Lu, V. V. Strelets, M. F. Ryan, W. J. Pietro and A. B. P. Lever, *Inorg. Chem.*, 1996, **35**, 1013.